Cell Reports, Volume *38*

Supplemental information

MAPK signaling and a mobile scaffold complex regulate AMPA receptor transport to modulate synaptic strength

Frédéric J. Hoerndli, Penelope J. Brockie, Rui Wang, Jerry E. Mellem, Angy Kallarackal, Rachel L. Doser, Dayton M. Pierce, David M. Madsen, and Andres V. Maricq

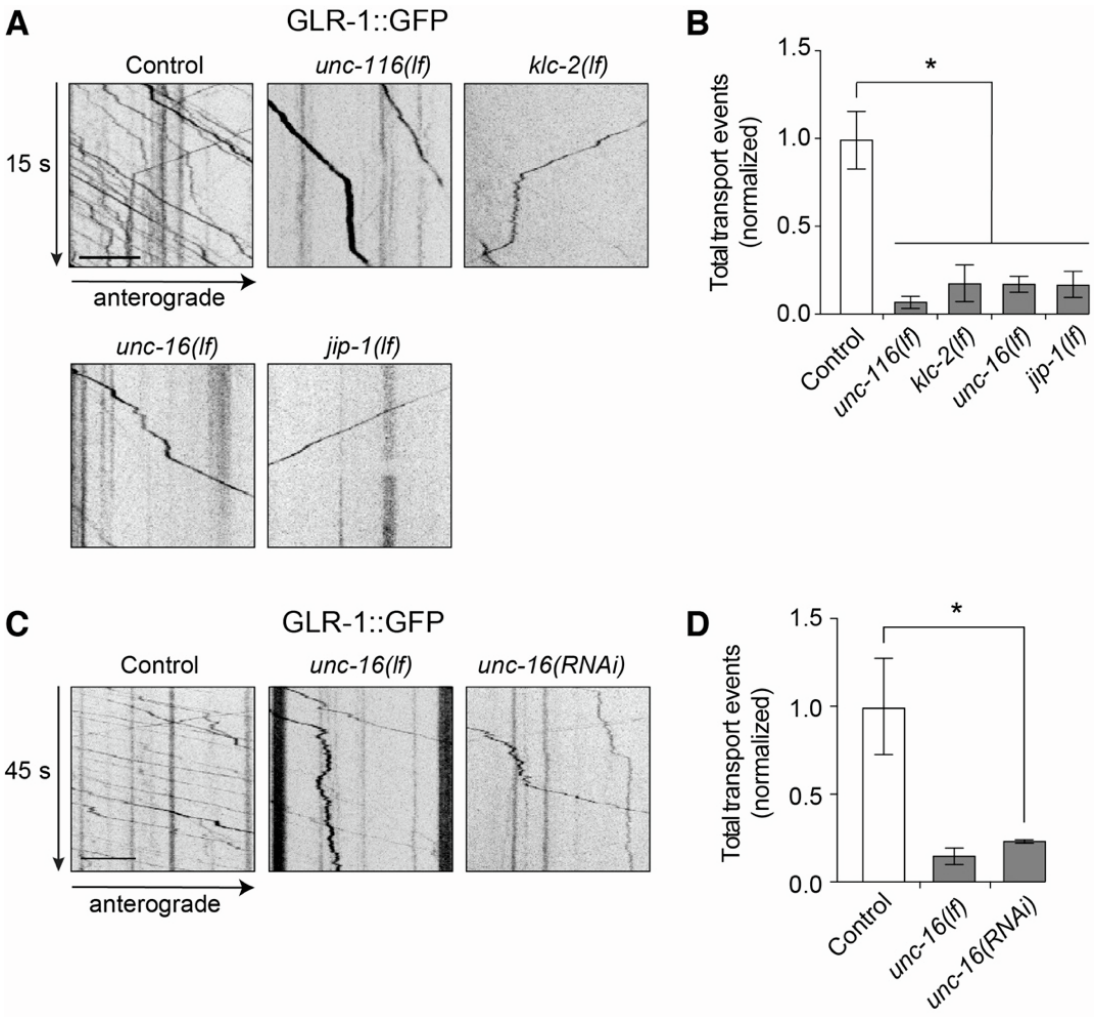

Figure S1. Scaffold-protein mutants phenocopy motor-protein mutants. Related to Figure 1.

(A) Kymographs of GLR-1::GFP transport in the AVA processes of transgenic control worms, and *unc-116(rh24)*, *klc-2(km11), unc-16(e109)* and *jip-1(km18)* loss-of-function (*lf*) mutants. (B) Total (anterograde and retrograde) transport events in control worms (n=10), *unc-116(lf)* (n=7), *klc-2(lf)* (n = 9), *unc-16(lf)* (n = 6), *and jip-1(lf)* (n = 4). (C) Kymographs of GLR-1::GFP transport in transgenic control worms, *unc-16(e109)*, and a transgenic strain that expressed *unc-16* double-stranded RNA (RNAi) in AVA only. (D) Total transport events in control worms (n=5), *unc-16(lf)* (n = 4) and *unc-16(RNAi)* (n = 5).

* $p < 0.05$ by Kruskal-Wallis test and Dunn's multiple testing correction. Error bars indicate SEM. Scale bars, 5 μm. All strains carried the *glr-1(ky176)* mutation.

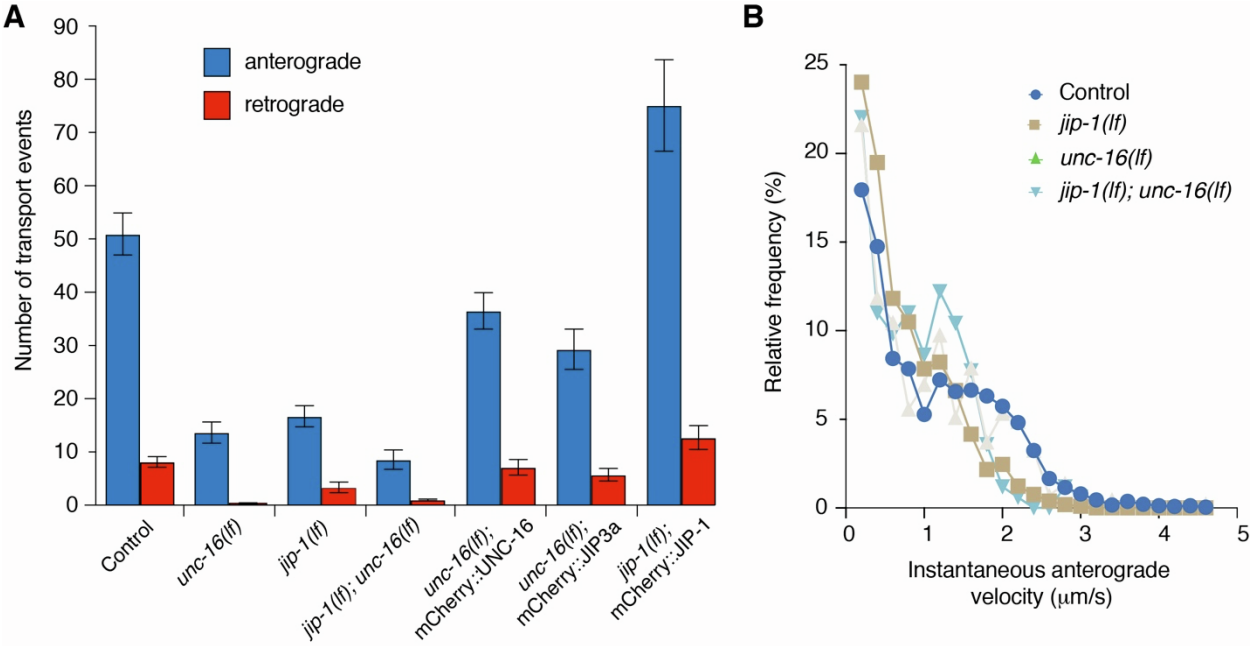

Figure S2. Anterograde and retrograde transport events, but not transport velocity, are modified in scaffold-protein mutants. Related to Figure 1.

(A) The number of GLR-1::GFP anterograde (blue) and retrograde (red) transport events observed during a 113 s interval in transgenic control worms (n = 15), *unc-16(lf)* (n = 12), *jip-1(lf)* (n = 14), *jip-1(lf); unc-16(lf)* (n = 9), *unc-16(lf);* mCherry::UNC-16 (n = 14), *unc-16(lf);* mCherry::JIP3a (n = 7) and *jip-1(lf)*; mCherry::JIP-1 (n = 10). Anterograde and retrograde transport in *unc-16(lf)* and *jip-1(lf)* single mutants, and *jip-1(lf); unc-16(lf)* double mutants were significantly different from control, $p < 001$; and anterograde and retrograde transport in *unc-16(lf);* mCherry::UNC-16, *unc-16(lf);* mCherry::JIP3a, and *jip-1(lf);* mCherry::JIP-1 were not significantly different from control using ANOVA with Kruskal-Wallis and Dunn's multiple testing. Error bars indicate SEM. (B) Relative frequency distribution of all velocities (anterograde and retrograde) of GLR-1::GFP transport described in Figure 1A and 1B, analyzed using KymoAnalyzer (see STAR Methods). The relative frequency represent data from the following number of velocity segments for each genotype: control (n = 2407), *jip-1(lf)* (n =

1057), *unc-16(lf)* (n = 430), *jip-1(lf); unc-16(lf)* (n = 336). Bin = 0.2 μm/s.

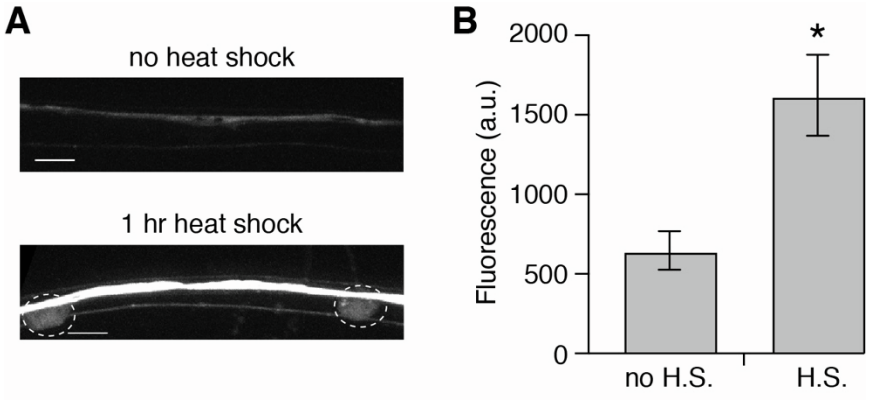

Figure S3. Heat-shock induced expression of mCherry::JIP-1. Related to Figures 1 and 2.

(A) Maximum projection confocal images of mCherry fluorescence before (top) and after (bottom) heat-shock (H.S.) induced expression of mCherry::JIP-1 in a transgenic worm that carried a *hsp16-2p::mCherry::jip-1* transgene. (Note: The transgenic strain also carried a *flp-18p::mCherry* transgene that expressed soluble mCherry in AVA.) Dotted circles indicate heat-shock induced expression of mCherry::JIP-1 in neuronal cell bodies. Scale bars, 5 μm. (B) Quantification of mCherry fluorescence in the ventral nerve cord of transgenic worms either before (no H.S.; n = 6) or after (H.S.; n = 8) heat-shock treatment. * $p < 0.01$ using a Student's t-test. Error bars indicate SEM.

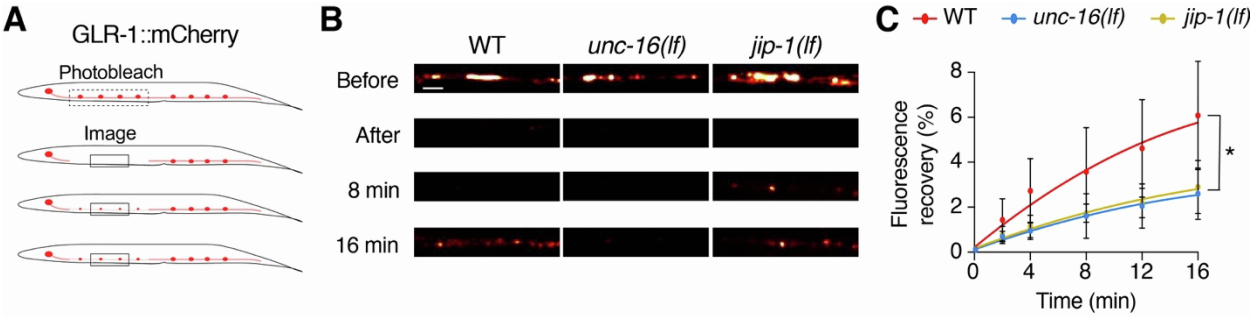

Figure S4. The rate of fluorescence recovery after photobleaching is slower in the scaffold-protein mutants. Related to Figure 3.

(A) Diagram showing the approximate region of the proximal AVA processes where GLR-1::mCherry was photobleached (dashed rectangle), and the region imaged after photobleaching (rectangle). Photobleaching was performed as previously described (see STAR Methods). (B) Images of GLR-1::mCherry before, immediately after (After) and either 8 or 16 minutes after photobleaching. Scale bar, 5 μm. (C) Quantification of the fluorescence recovery after photobleaching as a percentage of the signal before photobleaching; n = 8 for all genotypes. * $p < 0.01$, with a least mean square test between non-linear curve fits. Error bars indicate SEM. All strains carried the *glr-1(ky176)* mutation.

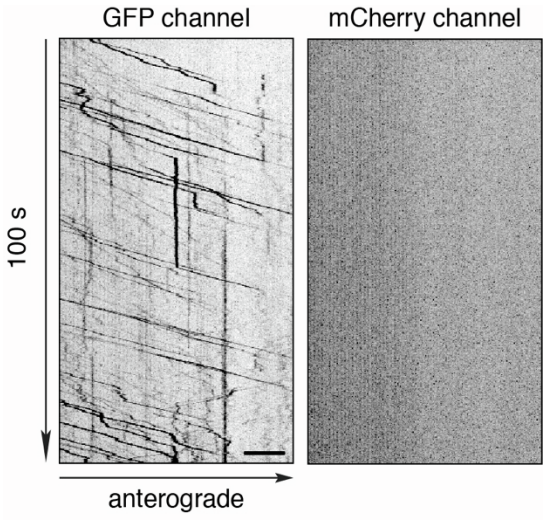

Figure S5. Absence of bleed-through signal during dual-channel acquisition. Related to Figure 4.

Kymographs showing transport events in the AVA processes of a transgenic worm that expressed GLR-1::GFP. The kymographs were generated from streaming movies captured using the same dual-channel acquisition protocol as that used to generate Figures 4A and 4B (see STAR Methods). No fluorescent signal was detected in the mCherry channel indicating that there was no bleed through of the GFP signal. Scale bar, 5 μm.

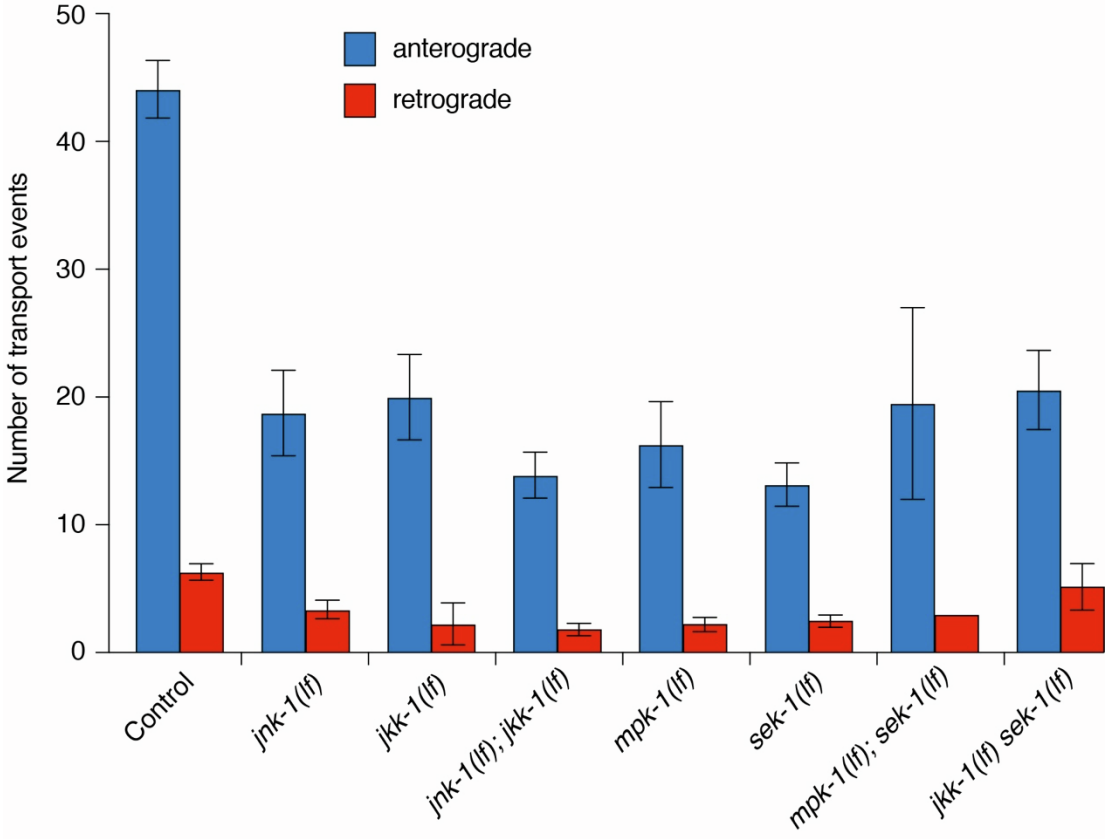

Figure S6. Anterograde and retrograde transport events are modified in MAPK-signaling mutants. Related to Figures 5 and 7.

(A) The number of GLR-1::GFP anterograde (blue) and retrograde (red) transport events observed during a 113 s interval in transgenic control worms (n = 13), *jnk-1(lf)* (n = 8), *jkk-1(lf)* (n = 4), *jnk-1(lf); jkk-1(lf)* (n = 9), *mpk-1(lf)* (n = 7), *sek-1(lf)* (n = 13), *mpk-1(lf); sek-1(lf)* (n = 2) and *jkk-1(lf) sek-1(lf)* (n = 9). Anterograde transport in all single and double mutants was significantly different from control, $p < 001$. Retrograde transport was significantly different from control ($p < 0.01$) in *jnk-1(lf); jkk-1(lf)* and *sek-1(lf)*, $p < 001$. All statistics were analyzed using ANOVA with Kruskal-Wallis and Dunn's multiple testing. Error bars indicate SEM.

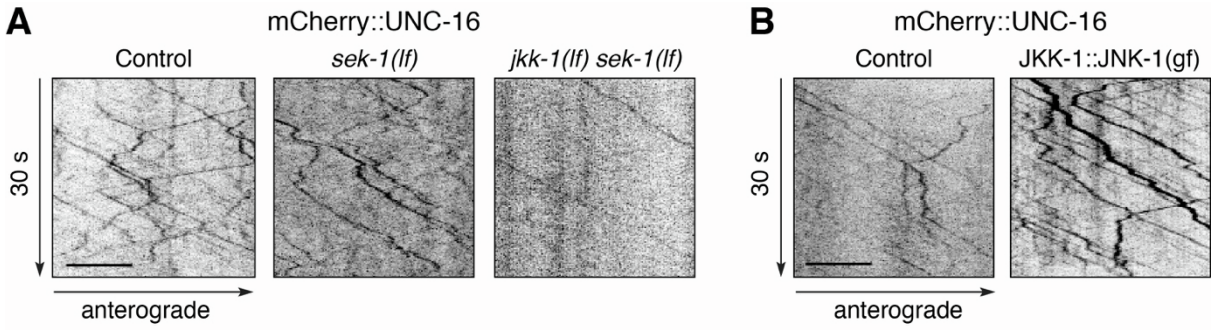

Figure S7. mCherry::UNC-16 transport is modified in MAPK-signaling mutants. Related to Figure 7.

(A) Kymographs of mCherry::UNC-16 transport (quantified in Figure 7I) in control worms, and *sek-1(lf)* and *jkk-1(lf) sek-1(lf)* mutants. (B) Kymographs of mCherry::UNC-16 transport (quantified in Figure 7J) in control worms and transgenic worms that expressed JKK-1::JNK-1(gf).

Scale bars, 5 μm.

Table S1. Description of mutant alleles. Related to Figures 1–7, S1 and S2

Gene	Allele	Mutation	Reference
glr-1	*ky176*	1.6 kb deletion	Maricq et al., 1995, Nature
unc-16	*e109*	448 bp deletion	Byrd et al., 2001, Neuron
jip-1	*km18*	1028 bp deletion	Erik Jorgensen, personal communication
unc-116	*rh24*	E388K; I304M	Patel et al., 1993, PNAS
klc-2	*km11*	1.5 kb deletion; and duplication with C-terminal deletion on LG V	Sakamoto et al., 2005, Mol Bio Cell
unc-43	*n498n1186(lf)*	E108K; Q138*	Park and Horvitz, 1986, Genetics; Rongo and Kaplan, 1999, Nature
unc-43	*n498sd(gf)*	E108K	Park and Horvitz, 1986, Genetics; Rongo and Kaplan, 1999, Nature
jnk-1	*gk7*	1.2 kb deletion	Villanueva, 2001, EMBO
jkk-1	*km2*	970 bp deletion	Kawasaki et al., 1999, EMBO
sek-1	*km4*	2.1 kb deletion	Tanaka-Hino et al., 2002, EMBO
mpk-1	*oz140*	W351*	Lackner and Kim, Genetics, 1998

Table S2. Primer sequences used for genotyping and for *unc-16(dsRNAi)*. Related to Figures 1–7, S1 and S2.

Gene	Allele	Forward primer	Reverse primer
glr-1	*ky176*	5'-CTGTCGATCCGCCACCTTGAATTC-3'	5'-GACCGCAATTGTGAAACATTTTGG-3'
unc-16	*e109*	5'-TGACTGTTGTGTCGTTGTTTGTAG-3'	5'-GCTTCTTCCTCTTCTGATTGTTTC-3'
jip-1	*km18*	5'-ACACGTTGACCGGACTGC-3'	5'-CCCGCAACCTATTTCTTATC-3'
klc-2	*km11*	5'-GTTGGACCACAACCAGTCAC-3'	5'-CAGTTTGAGATGTGCTCGTTG-3'
jnk-1	*gk7*	5'-ATCAATCATTCGAGGAACCCGTGG-3'	5'-GCCCGATAGTATCTTGTCACAACG-3'
jkk-1	*km2*	5'-GCTCTTCCACATCTTCAAGTCCTC-3'	5'-GCATGATCAAGCCGAAACTAGTAG-3'
sek-1	*km4*	5'-AGACGACACACTGATTGCCTTTTG-3'	5'-ATGAAATAAGGATAAGCGGTTGAC-3'
unc-16	*dsRNAi*		
	Pf–Prs	5'-CGAGTTTGTTGGAGCAAAACACGG-3'	5'-CTATGATTAGAAGTCTTCGTCTTTTTCTCTAACCCTGAAATTATTATTTTTAGTTG-3'
	Pf–Pra	5'-CGAGTTTGTTGGAGCAAAACACGG-3'	5'-GCAGAACTTCCGATCCTCTCAAAATTCTAACCCTGAAATTATTATTTTTAGTTG-3'
	Tf–Tr	5'-GAAAAAGACGAAGACTTCTAATCATAG-3'	5'-ATTTTGAGAGGATCGGAAGTTCTGC-3'
	Pf–Tr**	5'-TGTCACATACTGCTCGAATCGGAG-3'	5'-CGACTTCCCAGATAATCAAATGTG-3'
	Pf–Tf**	5'-TGTCACATACTGCTCGAATCGGAG-3'	5'-CCGGAGTTAGAAGATGAAATTAAGAG-3'